



A parametric study of assembly pressure, thermal expansion, and membrane swelling in PEM fuel cells

Maher A.R. Sadiq Al-Baghdadi

Fuel Cell Research Center, International Energy and Environment Foundation, Najaf, P.O.Box 39, Iraq.

Abstract

Proton Exchange membrane (PEM) fuel cells are still undergoing intense development, and the combination of new and optimized materials, improved product development, novel architectures, more efficient transport processes, and design optimization and integration are expected to lead to major gains in performance, efficiency, durability, reliability, manufacturability and cost-effectiveness.

PEM fuel cell assembly pressure is known to cause large strains in the cell components. All components compression occurs during the assembly process of the cell, but also during fuel cell operation due to membrane swelling when absorbs water and cell materials expansion due to heat generating in catalyst layers. Additionally, the repetitive channel-rib pattern of the bipolar plates results in a highly inhomogeneous compressive load, so that while large strains are produced under the rib, the region under the channels remains approximately at its initial uncompressed state. This leads to significant spatial variations in GDL thickness and porosity distributions, as well as in electrical and thermal bulk conductivities and contact resistances (both at the ribe-GDL and membrane-GDL interfaces). These changes affect the rates of mass, charge, and heat transport through the GDL, thus impacting fuel cell performance and lifetime.

In this paper, computational fluid dynamics (CFD) model of a PEM fuel cell has been developed to simulate the pressure distribution inside the cell, which are occurring during fuel cell assembly (bolt assembling), and membrane swelling and cell materials expansion during fuel cell running due to the changes of temperature and relative humidity. The PEM fuel cell model simulated includes the following components; two bi-polar plates, two GDLs, and, an MEA (membrane plus two CLs). This model is used to study and analyses the effect of assembling and operating parameters on the mechanical behaviour of PEM. The analysis helped identifying critical parameters and shed insight into the physical mechanisms leading to a fuel cell durability under various operating conditions. The model is shown to be able to understand the effect of pressure distribution inside the cell on the performance and durability that have limited experimental data.

Copyright © 2016 International Energy and Environment Foundation - All rights reserved.

Keywords: PEM fuel cell; CFD; Clamping pressure; Assembly and accumulation errors; Inhomogeneous compression.

1. Introduction

1.1. Durability

Durability is one of the most critical remaining issues impeding successful commercialization of broad PEM fuel cell stationary and transportation energy applications, and the durability of fuel cell stack

components remains, in most cases, insufficiently understood [1-10]. Lengthy required testing times, lack of understanding of most degradation mechanisms, and the difficulty of performing in-situ, non-destructive structural evaluation of key components makes the topic a difficult one [11, 12].

The Membrane-Electrode-Assembly (MEA) is the core component of PEM fuel cell and consists of membrane with the gas diffusion layers (GDL) including the catalyst layers (CL) attached to each side. The fuel cell MEA durability plays a vital role in the overall lifetime achieved by a stack in field applications. Within the MEA's electrocatalyst layers are three critical interfaces that must remain properly intermingled for optimum MEA performance: platinum/carbon interface (for electron transport and catalyst support); platinum/Nafion interface (for proton transport); and Nafion/carbon interface (for high-activity catalyst dispersion and structural integrity). The MEA performance shows degradation over operating time, which is dependent upon materials, fabrication and operating conditions [13, 14].

Durability is a complicated phenomenon; linked to the chemical and mechanical interactions of the fuel cell stack components, i.e. electro-catalysts, membranes, gas diffusion layers, bipolar plates, and end plates, under severe environmental conditions, such as elevated temperature and low humidity [15]. In fuel cell systems, failure may occur in several ways such as chemical degradation of the ionomer membrane or mechanical failure in the PEM that results in gradual reduction of ionic conductivity, increase in the total cell resistance, and the reduction of voltage and loss of output power [16]. Mechanical degradation is often the cause of early life failures. Mechanical damage in the PEM can appear as through-the-thickness flaws or pinholes in the membrane, or delaminating between the polymer membrane and gas diffusion layers [17, 18].

Mechanical stresses which limit MEA durability have two origins. Firstly, this is the stresses arising during fuel cell assembly (bolt assembling). The bolts provide the tightness and the electrical conductivity between the contact elements. Secondly, additional mechanical stresses occur during fuel cell running because PEM fuel cell components have different thermal expansion and swelling coefficients. Thermal and humidity gradients in the fuel cell produce dilatations obstructed by tightening of the screw-bolts. Compressive stress increasing with the hygro-thermal loading can exceed the yield strength which causes the plastic deformation. The mechanical behaviour of the membrane depends strongly on hydration and temperature [19, 20].

Water management is one of the critical operation issues in PEM fuel cells. Spatially varying concentrations of water in both vapour and liquid form are expected throughout the cell because of varying rates of production and transport. Devising better water management is therefore a key issue in PEM fuel cell design, and this requires improved understanding of the parameters affecting water transport in the membrane [21, 22]. Thermal management is also required to remove the heat produced by the electrochemical reaction in order to prevent drying out of the membrane, which in turn can result not only in reduced performance but also in eventual rupture of the membrane [23, 24]. Thermal management is also essential for the control of the water evaporation or condensation rates [25]. As a result of in the changes in temperature and moisture, the PEM, gas diffusion layers (GDL), and bipolar plates will all experience expansion and contraction. Because of the different thermal expansion and swelling coefficients between these materials, hygro-thermal stresses are expected to be introduced into the unit cell during operation. In addition, the non-uniform current and reactant flow distributions in the cell can result in non-uniform temperature and moisture content of the cell, which could in turn, potentially causing localized increases in the stress magnitudes. The need for improved lifetime of PEM fuel cells necessitates that the failure mechanisms be clearly understood and life prediction models be developed, so that new designs can be introduced to improve long-term performance. Increasing of the durability is a significant challenge for the development of fuel cell technology. Membrane failure is believed to be the result of combined chemical and mechanical effects acting together [11, 12, 15]. Variations in temperature and humidity during operation cause stresses and strains (mechanical loading) in the membrane as well as the MEA and is considered to be the mechanical failure driving force in fuel cell applications [16-20]. Reactant gas cross over, hydrogen peroxide formation and movement, and cationic contaminants are all to be major factors contributing to the chemical decomposition of polymer electrolyte membranes. While chemical degradation of membranes has been investigated and reported extensively in literature [11-18], there has been little work published on mechanical degradation of the membrane. Investigating the mechanical response of the membrane subjected to change in humidity and temperature requires studying and modelling of the stress-strain behaviour of membranes and MEAs. Weber and Newman [26] developed one-dimensional model to study the stresses development in the fuel cell. They showed that hygro-thermal stresses might be an important reason for membrane failure, and

the mechanical stresses might be particularly important in systems that are non-isothermal. However, their model is one-dimensional and does not include the effects of material property mismatch among PEM, GDL, and bipolar plates.

Tang et al. [27] studied the hygro and thermal stresses in the fuel cell caused by step-changes of temperature and relative humidity. Influence of membrane thickness was also studied, which shows a less significant effect. However, their model is two-dimensional, where the hygro-thermal stresses are absent in the third direction (flow direction). In addition, a simplified temperature and humidity profile with no internal heat generation were assumed, (constant temperature for each upper and lower surfaces of the membrane was assumed).

Kusoglu et al. [28] developed two-dimensional model to investigate the mechanical response of a PEM subjected to a single hygro-thermal loading cycle, simulating a simplified single fuel cell duty cycle. A linear, uncoupled, simplified temperature and humidity profile with no internal heat generation, assuming steady-state conditions, was used for the loading and unloading conditions. Linear-elastic, perfectly plastic material response with temperature and humidity dependent material properties was used to study the plastic deformation behaviour of the membrane during the cycle. The stress evolution during a simplified operating cycle is determined for two alignments of the bipolar plates. They showed that the alternating gas channel alignment produces higher shear stresses than the aligned gas channel. Their results suggested that the in-plane residual tensile stresses after one fuel cell duty cycle developed upon unloading, may lead to the failure of the membranes due to the mechanical fatigue. They concluded that in order to acquire a complete understanding of these damage mechanisms in the membranes, mechanical response under continuous hygro-thermal cycles should be studied under realistic cell operating conditions.

Kusoglu et al. [29] investigated the mechanical response of polymer electrolyte membranes in a fuel cell assembly under humidity cycles at a constant temperature. The behaviour of the membrane under hydration and dehydration cycles was simulated by imposing a simplified humidity gradient profile from the cathode to the anode. Also, a simplified temperature profile with no internal heat generation were assumed. Linear elastic, plastic constitutive behaviour with isotropic hardening and temperature and humidity dependent material properties were utilized in the simulations for the membrane. The evolution of the stresses and plastic deformation during the humidity cycles were determined using two-dimensional finite elements model for various levels of swelling anisotropy. They showed that the membrane response strongly depends on the swelling anisotropy where the stress amplitude decreases with increasing anisotropy. Their results suggested that it may be possible to optimize a membrane with respect to swelling anisotropy to achieve better fatigue resistance, potentially enhancing the durability of fuel cell membranes.

Solasi et al. [30] developed two-dimensional model to define and understand the basic mechanical behaviour of ionomeric membranes clamped in a rigid frame, and subjected to changes in temperature and humidification. Expansion/contraction mechanical response of the constrained membrane as a result of change in hydration and temperature was also studied in non-uniform geometry. A circular hole in the centre of the membrane can represent pinhole creation or even material degradation during fuel cell operation was considered as the extreme form of non-uniformity in this constraint configuration. Their results showed that the hydration have a bigger effect than temperature in developing mechanical stresses in the membrane. These stresses will be more critical when non-uniformity as a form of hydration profile or a physical pinhole exists across the membrane.

Bogachev et al. [31] developed a linear elastic-plastic two-dimensional model of fuel cell with hardening for analysis of mechanical stresses in MEA arising in cell assembly procedure. The model includes the main components of real fuel cell (membrane, gas diffusion layers, graphite plates, and seal joints) and clamping elements (steel plates, bolts, nuts). The stress and plastic deformation in MEA are simulated taking into account the realistic clamping conditions. Their results concluded that important variations of stresses generated during the assembling procedure can be a source of the limitation of the mechanical reliability of the system.

Suvorov et al. [32] analyzed the stress relaxation in the membrane electrode assemblies (MEA) in PEM fuel cells subjected to compressive loads using numerical simulations (finite element method). This behaviour is important because nonzero contact stress is required to maintain low electric resistivity in the fuel cell stack. In addition to the two-dimensional assumption, the temperature was kept fixed and equal to the operating temperature at all time. All properties were considered to be independent of the temperature. They showed that under applied compressive strains the contact stress in the membrane

electrode assembly (MEA) will drop with time. The maximum contact stress and the rate of stress relaxation depend on the individual properties of the membrane and the gas diffusion layer.

Tang et al. [33] examined the hygro-thermo-mechanical properties and response of a class of reinforced hydrated perfluorosulfonic acid membranes (PFSA) in a fuel cell assembly under humidity cycles at a constant temperature. The load imposed keeps the membrane at elevated temperature (85 C) and linearly cycles the relative humidity between the initial (30% RH) and the hydrated state (95% RH) at the cathode side of membrane. The evolution of hygro-thermally induced mechanical stresses during the load cycles were determined for reinforced and unreinforced PFSA membranes using two-dimensional finite elements model. Their numerical simulations showed that the in-plane stresses for reinforced PFSA membrane remain compressive during the cycling. Compressive stresses are advantageous with respect to fatigue loading, since compressive in-plane stresses will significantly reduce the slow crack growth associated with fatigue failures. They showed that the reinforced PFSA membrane exhibits higher strength and lower in-plane swelling than the unreinforced PFSA membrane used as a reference, therefore, should result in higher fuel cell durability.

Bogachev et al. [34] developed two-dimensional model to study the evolution of stresses and plastic deformations in the membrane during the turn-on phase. They showed that the maximal stresses in the membrane take place during the humidification step before the temperature comes to its steady-state value. The magnitude of these stresses is sufficient for initiation of the plastic deformations in the Nafion membrane. The plastic deformations in the membrane develop during the entire humidification step. At the steady state the stresses have the highest value in the centre of the membrane; the Mises stress is equal to 2.5 MPa.

In addition to the two-dimensional assumption, the operating conditions have been taken into account by imposing the heating sources as a simplified directly related relationship between power generation and efficiency of the fuel cell. The moisture is set gradually from an initial value of 35% up to 100%. The humidity is imposed after all heat sources reach steady state. The imposed moisture is assumed to be uniformly distributed in the membrane during turn-on stage (before reaching the steady state). However, this questionable assumption leads to overestimation of the maximal stresses in the membrane during turn-on stage.

Al-Baghdadi [35] incorporated the effect of hygro and thermal stresses into non-isothermal three-dimensional CFD model of PEM fuel cell to simulate the hygro and thermal stresses in one part of the fuel cell components, which is the polymer membrane. They studied the behaviour of the membrane during the operation of a unit cell. The results showed that the displacement have the highest value in the centre of the membrane near the cathode side inlet area.

In order to acquire a complete understanding of the damage mechanisms in the membrane and gas diffusion layers, mechanical response under steady-state hygro-thermal stresses should be studied under real cell operating conditions and in real cell geometry.

1.2. PEM fuel cell assembly

The stacking design and cell assembly parameters significantly affect the performance of fuel cells [36]. Adequate contact pressure is needed to hold together the fuel cell stack components to prevent leaking of the reactants, and minimize the contact resistance between layers. The required clamping force is equal to the force required to compress the fuel cell layers adequately while not impeding flow. The assembly pressure affects the characteristics of the contact interfaces between components. If inadequate or nonuniform assembly pressure is used, there will be stack-sealing problems, such as fuel leakage, internal combustion, and unacceptable contact resistance. Too much pressure may impede flow through the GDL, or damage the MEA, resulting in a broken porous structure and a blockage of the gas diffusion passage. In both cases, the clamping pressure can decrease the cell performance. Every stack has a unique assembly pressure due to differences in fuel cell materials and stack design. Due to thin dimensions and the low mechanical strength of the electrodes and electrolyte layer versus the gaskets, bipolar plates, and end plates, the most important goal in the stack design and assembly is to achieve a proper and uniform pressure distribution [37].

The most common method of clamping the stack is by using bolts. When considering the optimal clamping pressure on the properties of the fuel cell stack, sometimes an overlooked factor is the torque required for the bolts, and the factors that contribute to the ideal torque. The optimal torque is not merely due to the ideal clamping pressure on the fuel cell layers, but it is also affected by the shape and material of the bolt and nut, the bolt seating and threading, the stack layers, thickness, and number of layers.

Materials bolted together withstand moment loads by clamping the surfaces together, where the edge of the part acts as a fulcrum, and the bolt acts as a force to resist the moment created by an external force or moment [37].

The contact resistance and GDL permeability are governed by the material properties of the contacting GDL and bipolar plate layers. The contact resistance between the catalyst and membrane layers is low because they are fused together, and the contact resistance between the bipolar plates and other layers is low because the materials are typically nonporous with similar material properties (high density, with similar Poisson's ratios and Young's modulus). The GDL and the bipolar plate layers have several characteristics that make the contact resistance and permeability larger than between the other layers: (1) the Poisson's ratios and Young's modulus have large differences (a hard material with a soft material); (2) the GDL layer is porous, and the permeability has been reduced due to the reduction in pore volume or porosity; and (3) part of the GDL layer blocks the flow channels that are in the bipolar plate creating less permeability through the GDL as the compression increases [38, 39].

Vibration characteristics are required to understand the vibration behaviour of PEM fuel cell stack components such as the membrane, catalyst layer, gas diffusion layers, and bi-polar plates. Vibrating at resonance frequency can lead to the initiation and acceleration of defect formation, which may ultimately result in operational failure. Furthermore, during the running of a PEM fuel cell stack, the unavoidable vibration may aggravate the assembly error, especially for the automotive application due to more vibrations. Vibrations may exacerbate defects such as pinholes, cracks, and delamination, which can result in fuel crossover, performance degradation, and reduced durability [40].

Su et al. [41] studied the effects of compression force on PEM fuel cell performance. A scanning electron microscope (SEM, JSM-5610LV; JEOL) was employed to observe the changes in the GDL surface microstructure compressed by the rib area of the bipolar plate. Figure 1 shows a cross-section of a single cell, showing two gas channels and one rib in the image. After the fuel cell is assembled, the physical characteristics of the compressed area of the GDL become different than those of the uncompressed area. The GDL surface of the area that is exposed to the rib clearly contains more cracks. In Figure 1, the GDL exposed to the gas channel is not under compression and only a small portion protrudes into the channel. Under the rib of the bipolar plate, the GDL is thinner than the channel portion.

Totzke et al. [42] studied the microstructure of carbon fiber-based GDL materials at different degrees of compression using synchrotron X-ray imaging. The superior brilliance of a synchrotron X-ray beam and the high spatial resolution of the associated imaging instrument were exploited to generate tomographic data that reproduce even smallest morphological details of the fiber material with great accuracy. This information was used to estimate some effects of the microstructure on both gas and liquid transport. Figure 2 clearly demonstrates that individual fiber endings protrude into the flow-field channel. These fibers are bent at the edges of the flow-field channel profile and tilt up with increasing degree of compression. At a compression degree of 29% some fiber endings protrude 295 nm into the channel volume where they potentially influence the gas flow and form obstacles for water droplets that are transported through the flow field channel.

Baik et al. [43] investigated the effects of the anisotropic bending stiffness of GDLs on the performance of polymer electrolyte membrane fuel cells with metallic bipolar plates. The cross-sectional images of GDLs upon compression were measured to compare the degree of intrusion of GDLs. Figure 3 shows the cross-sectional morphology of the GDL upon compression pressure at 1.52 MPa. As shown in figure, the trend of GDL intrusion into the channel. It was shown that variation in the cathode channel depth should affect the observed cell behavior more than that in the anode channel depth.

Nitta et al. [44] studied the effects of inhomogeneous compression of GDLs on local transport phenomena within a PEM fuel cell. A typical carbon paper or cloth GDL is soft and flexible and, therefore, when the GDL was compressed between two flow field plates it is deformed and intrudes into the channel as shown in Figure 4. Variations in GDL thickness and porosity due to compression affect the local transport phenomena since gas permeability, electric conductivity and electric and thermal contact resistances at the interfaces with neighbouring components all depend on compression.

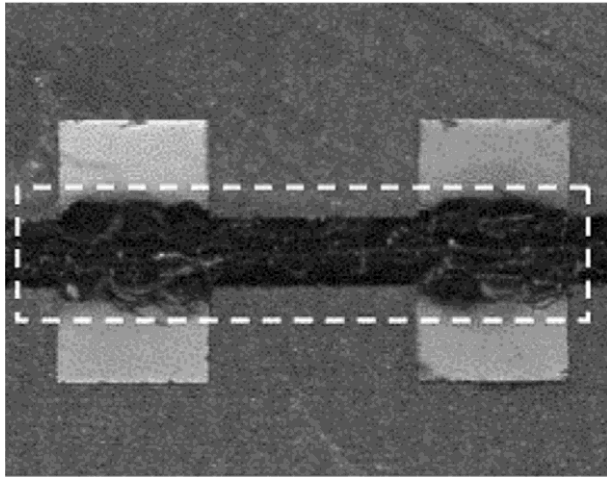


Figure 1. SEM photo of the assembled PEM fuel cell [41].

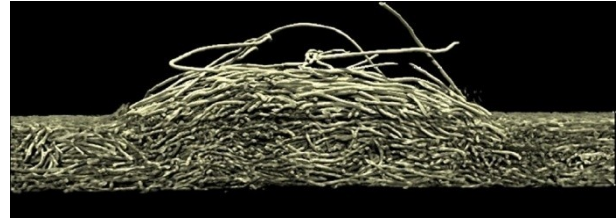


Figure 2. Perspective side-view illustrating the thickness of the GDL sample at a compression degree of 29% [42].



Figure 3. Cross-sectional morphology of GDLs upon compression [43].

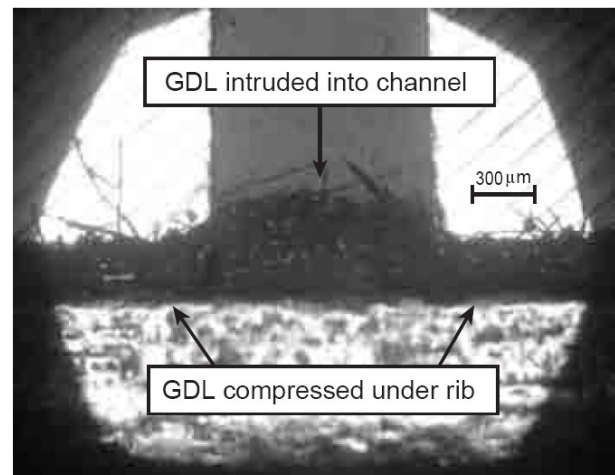


Figure 4. Cross-sectional view of the GDL (SGL 10 BA, SIGRACET®) taken by optical microscope (PMG3, Olympus) [44].

1.3. PEM fuel cell operation

The fuel cell stack is sized to generate the designed power output. PEM fuel cells show some losses of efficiency and power density with the scale up when the number of cells and their areas increase in a stack. As fuel cell manufacturing scales up, the relationship between fuel cell performance and design, manufacturing, and assembly processes must be well understood. Assembly pressure plays a significant role in determining fuel cell performance [36, 37]. During the assembly of a PEM fuel cell stack, GDL, bipolar plate, and membrane are clamped together using mechanical devices. A proper level of clamping pressure is needed to provide adequate gas sealing, as well as to reduce contact resistances at component interfaces. However, too high a pressure may over-compress the membrane and GDL, crushing their porous structures and cracking the bipolar plate. In addition, the electrical contact resistance, which constitutes a significant part of the ohmic resistance in a cell, especially when stainless steel, titanium or molded graphite is chosen as the bipolar plate material, can be significantly altered by clamping pressure and operating conditions [40, 41]. Assembly pressure makes the part of GDL under the land area be compressed and the part under channel area be protruded into channel cavity. This inhomogeneous compression causes unevenness of the material properties of GDL. The inhomogeneous deformation of

GDL as well as significant change of material properties influences fuel cell performance and durability dramatically [42].

PEM fuel cell stack assembly process, including clamping pressure, material properties of each component, design (component thickness and cell active area), and number of cells in the stack are important factors influencing the performance and durability of the PEM fuel cell stack. Furthermore, when temperature and relative humidity increase during operation, the membrane absorbs water and swells. Since the relative position between the top and bottom end plates is fixed, the polymer membrane is spatially confined. Thus the GDL will be further compressed under the land and the intrusion into channel becomes more significant [43, 44]. Assembly pressure, contact resistance, membrane swelling and operating conditions, etc., combine to yield an optimum assembly pressure.

2. PEM fuel cell model

2.1 Computational domain

A computational model of an entire cell would require very large computing resources and excessively long simulation times. The computational domain in this study is therefore limited to one straight flow channel with the land areas. The full computational domain consists of cathode and anode gas flow channels, and the membrane electrode assembly as shown in Figure 5. Material properties and dimensions of each component are shown in Table 1.

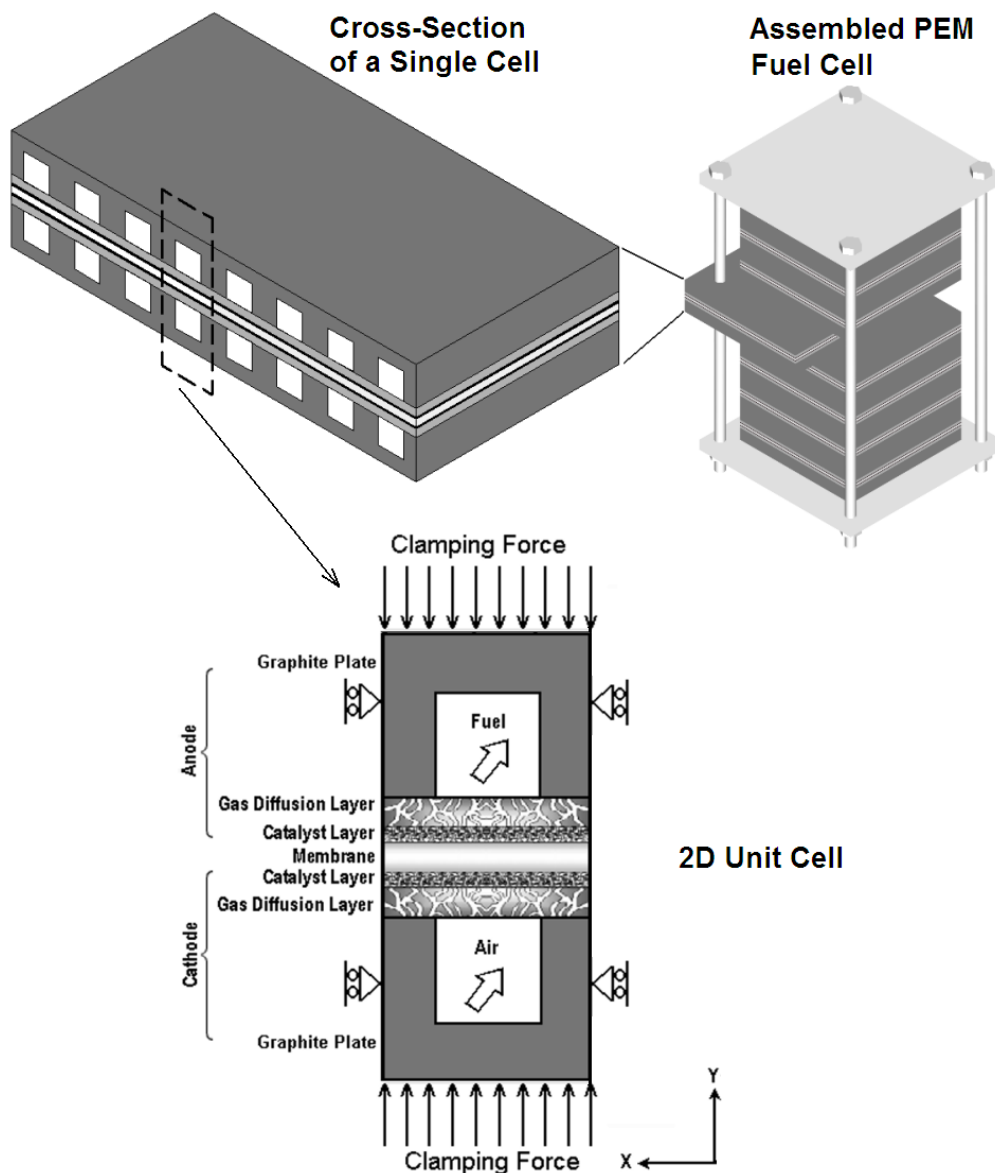


Figure 5. Computational domain.

Table 1. Properties and dimensions of the fuel cell components.

Property	Membrane	CL	GDL	Bipolar plate
Material	Nafion [®]	CCM	Carbon paper	Carbon graphite
Young's modulus [GPa]	Table 2	Table 2	10	10
Density [kg/m ³]	2000	2000	400	1800
Poisson's ratio	0.25	0.25	0.25	0.25
Expansion coefficient [K ⁻¹]	123e ⁻⁶	123e ⁻⁶	-0.8e ⁻⁶	5e ⁻⁶
Conductivity [W m ⁻¹ K ⁻¹]	0.455	0.455	17.122	95
Specific heat [J kg ⁻¹ K ⁻¹]	1050	1050	500	750
Width [mm]	3	3	3	one channel: 1 mm two ribs: 1 mm each.
Thickness [mm]	0.24	0.03	0.26	channel height: 1mm plate: 1 mm

Table 2. Young's modulus at various temperatures and humidities of Nafion[®].

Young's modulus [MPa]	Relative humidity [%]			
	30	50	70	90
T=25 C	197	192	132	121
T=45 C	161	137	103	70
T=65 C	148	117	92	63
T=85 C	121	85	59	46

2.2. Solid mechanics model

PEM fuel cell assembly pressure is known to cause large strains in the cell components. All components compression occurs during the assembly process of the cell, but also during fuel cell operation due to membrane swelling when absorbs water and cell materials expansion due to heat generating in catalyst layers. Additionally, the repetitive channel-rib pattern of the bipolar plates results in a highly inhomogeneous compressive load, so that while large strains are produced under the rib, the region under the channels remains approximately at its initial uncompressed state. This leads to significant spatial variations in GDL thickness and porosity distributions, as well as in electrical and thermal bulk conductivities and contact resistances (both at the ribe-GDL and membrane-GDL interfaces). These changes affect the rates of mass, charge, and heat transport through the GDL, thus impacting fuel cell performance and lifetime.

2.2.1. Solid mechanics model during assembly

The mechanical strain induced in the components by the stacking and clamping process (assembly process) can be written from Hooke's law as [11, 35];

$$\pi_M = \frac{1+\nu}{E} \sigma_{ij} - \frac{\nu}{E} \delta_{ij} \sigma_{kk} \quad (1)$$

where E is Young's modulus, ν is the Poisson's ratio of the material, δ_{ij} denotes the Kronecker delta, σ_{ij} is the stress tensor, and $\sigma_{kk} = \sigma_{11} + \sigma_{22} + \sigma_{33}$.

2.2.2. Solid mechanics model during operation

When running fuel cell, temperature and humidity are play a critical factors in a fuel cell durability. Additional mechanical stresses occur during fuel cell running because PEM fuel cell components have different thermal expansion and swelling coefficients. Thermal and humidity gradients in the fuel cell produce dilatations obstructed by tightening of the screw-bolts.

The thermal strains resulting from a change in temperature of an unconstrained isotropic volume are given by [35];

$$\pi_T = \phi(T - T_{Ref}) \quad (2)$$

where ϕ is thermal expansion [1/K].

The swelling strains caused by moisture change in membrane are given by [35];

$$\pi_S = \lambda_{mem}(\mathfrak{R} - \mathfrak{R}_{Ref}) \quad (3)$$

where λ_{mem} is membrane humidity swelling-expansion and \mathfrak{R} is the relative humidity [%].

2.3. Compression of PEM fuel cell gas diffusion layers

During GDL compression, it is assumed that only its pore volume is compressed, whereas its solid volume remains unchanged. As a result, the GDL porosity is reduced and can be calculated as [38, 39];

$$\varepsilon = \frac{\varepsilon_0 - 1 + e^{vs}}{e^{vs}} \quad (4)$$

where ε_0 is the initial porosity, vs is the volumetric strain at each point.

One of the key factors that cause power loss in PEM fuel cells is the contact resistance between the bipolar plate and the gas diffusion layer, especially when stainless steel, titanium or molded graphite is used as the BPP material. Contact resistance is determined by the material properties, surface topology, clamping pressure and operation conditions. A high clamping pressure leads to an increase in the contact area between the bipolar plate and GDL, which in turn decreases the contact resistance. However, a large pressure may cause GDL to be over compressed which results in flow resistance increasing. Furthermore, a large pressure may deform the MEA causing cell leakage and internal short. Thus, it is important to investigate the contact behaviour between bipolar plate and GDL.

The contact resistance between the bipolar plate and the GDL, $R_{contact}$ [$\text{m}\Omega \text{cm}^2$] can be calculated from [38, 39];

$$R_{contact} = 2.2163 + \frac{3.5306}{P_{contact}} \quad (5)$$

where $P_{contact}$ is the contact pressure [MPa].

3. Computational grid

The governing equations were discretized using a finite-volume method and solved using an academic edition of multi-physics computational fluid dynamic (CFD) package. Stringent numerical tests were performed to ensure that the solutions were independent of the grid size. A computational quadratic mesh

consisting of a total of 14768 domain elements and 960 boundary elements was found to provide sufficient spatial resolution (Figure 6). The coupled set of equations was solved iteratively, and the solution was considered to be convergent when the relative error was less than 1.0×10^{-6} in each field between two consecutive iterations.

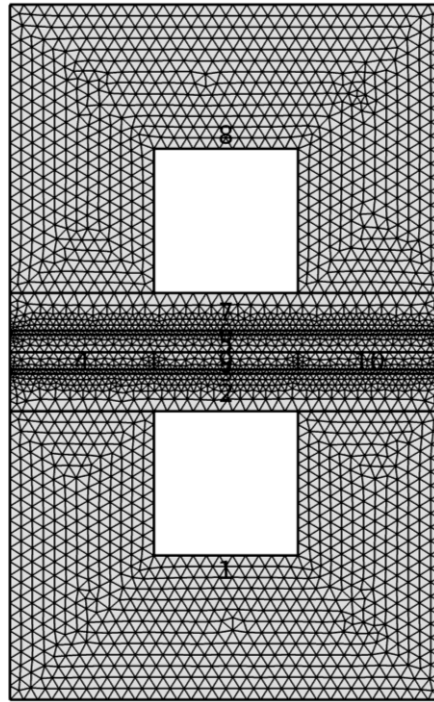


Figure 6. Computational mesh of a PEM fuel cell.

4. Results and discussion

4.1. PEM fuel cell analysis during assembly

The assembly conditions are set to reference temperature 20 C, and relative humidity 30%, where the thermal strain of the all fuel cell components and the swelling strain of the membrane are equals to zero. The clamping forces of the nut and bolt are applied on a specific area of the end plates in the assembly procedure. The clamping pressure of 1 MPa are used as the base case assembly conditions. Material properties of each component are shown in Table 1.

Figures 7-10 showing the analysis of the PEM fuel cell during assembly process at the base case conditions. Figure 7. shows the distribution of the total displacement in the PEM fuel cell during assembly process. The pressure distribution in the fuel cell that developed during the assembly process can be seen in Figure 8. The figure shows pressure distribution (contour plots) and deformation shape for the cell. The figure is clearly explain the effect of the repetitive channel-rib pattern on the pressure distribution.

In a real PEM fuel cell, the contact pressure on the GDL is different from the clamping pressure because of the channels in the bipolar plate. Furthermore, due to the round corners of the bipolar plate, the contact behaviour at the interface is hard to predict without a CFD analysis. Figure 9. shows the contact pressure between all layers of the fuel cell components during assembly process.

The stresses distribution in the fuel cell that developed during the assembly process can be seen in Figure 10. The figure shows von Mises stress distribution (contour plots) and deformation shape for the fuel cell.

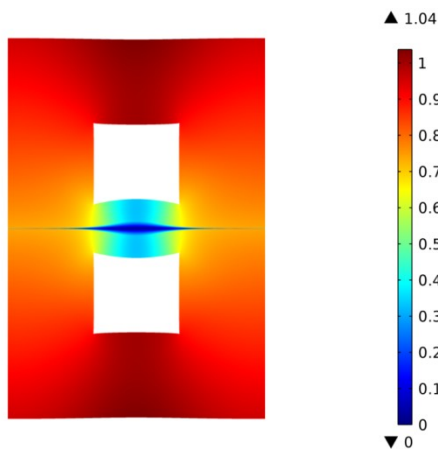


Figure 7. Total displacement [μm] in the PEM fuel cell during assembly process, (deformed shape plot, scale enlarged 200 times).

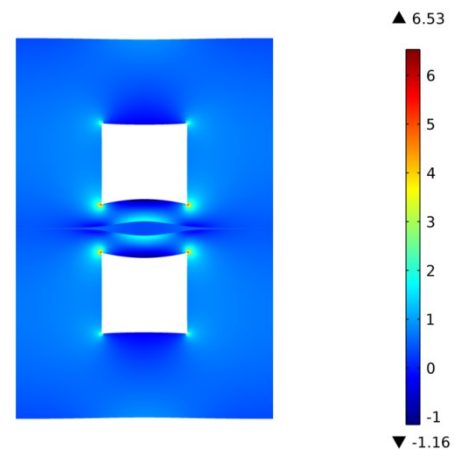


Figure 8. Pressure distribution [MPa] in the PEM fuel cell during assembly process, (deformed shape plot, scale enlarged 200 times).

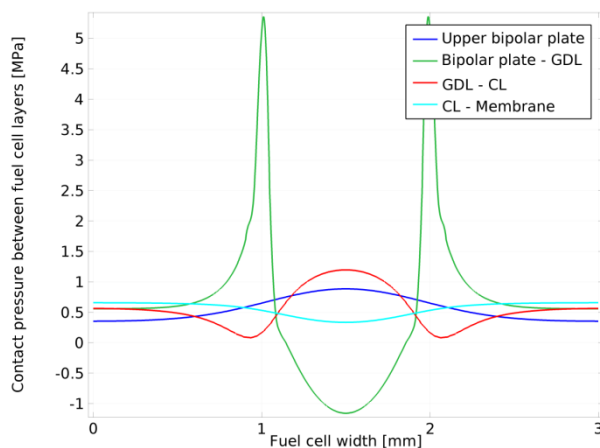


Figure 9. Contact pressure [MPa] between all layers of the fuel cell components during assembly process.

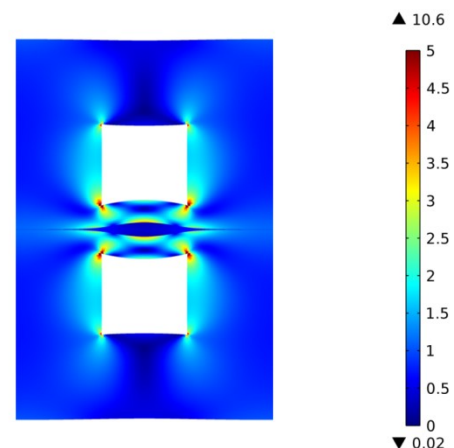


Figure 10. Mises stress distribution [MPa] in the PEM fuel cell during assembly process, (deformed shape plot, scale enlarged 200 times).

Several mechanical criteria are used to characterize the quality of the assembly. Results with different assembly conditions are discussed in the following subsections. In the following subsections only the parameter investigated is changed, all other parameters are at the base case conditions as outlined in Table 1.

4.1.1. Effect of clamping pressure

In PEM fuel cells, all components are generally assembled between clamping plates by applying a torque moment on the tightening bolts; as a consequence the clamping force plays an important role for stack realisation. The function of the stack-compression hardware is to fasten cell components with a defined and homogeneous pressure. If these requirements are not accurately fulfilled, the function and the durability of the cell will be influenced negatively. The MEAs and the bipolar plates need to be fixed in accurate positions and the compression of gaskets needs to be safe and homogeneous. If the pressure is too high, it will cause mechanical failure of the membrane or of the bipolar plate. Furthermore, an excessive compression of the components, in particular the GDL, increases the mass transport problems with a consequent reduction of cell performance and lifetime especially at high current density. If the pressure is too low, it may cause gas or cooling fluid leakage. Another effect of low compression is the increased contact resistance between the GDL and the bipolar plate, which will result in an inhomogeneous current distribution and thus in a reduced lifetime of the MEA. Figures 11-14 showing this effect.

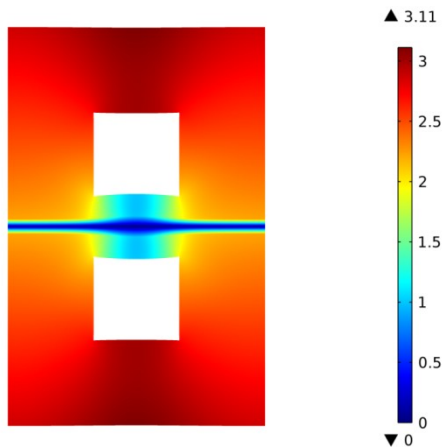


Figure 11. Total displacement [μm] in the PEM fuel cell during assembly process, (deformed shape plot, scale enlarged 200 times), (Clamping pressure = 3 MPa).

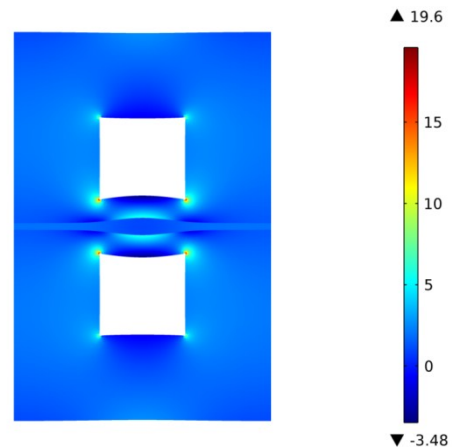


Figure 12. Pressure distribution [MPa] in the PEM fuel cell during assembly process, (deformed shape plot, scale enlarged 200 times), (Clamping pressure = 3 MPa).

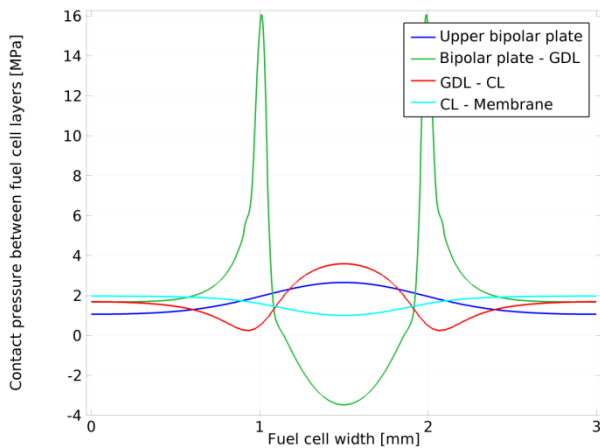


Figure 13. Contact pressure [MPa] between all layers of the fuel cell components during assembly process, (Clamping pressure = 3 MPa).

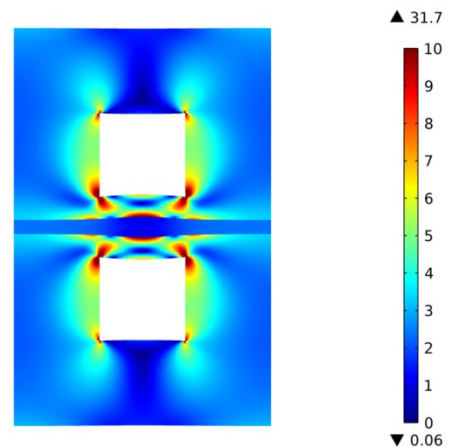


Figure 14. Mises stress distribution [MPa] in the PEM fuel cell during assembly process, (deformed shape plot, scale enlarged 200 times), (Clamping pressure = 3 MPa).

4.1.2. Effect of material properties of the cell components

The PEM fuel cell is a sandwich-like structure composed of many layers, materials and interfaces. The pressure distribution in PEM fuel cell therefore is affected by the component material properties, geometrical parameters and the clamping method. The effect of material variations on the cell layers pressure distribution is identified.

Bipolar plates have traditionally been fabricated from high-density graphite on account of its superior corrosion resistance, chemical stability, high thermal conductivity, and availability. However, due to its molecular structure, it exhibits poor mechanical properties, high manufacturing cost, and it is difficult to work with. Nevertheless, graphite has established itself as the benchmark material for fabrication of bipolar plates, against which all other materials are compared. However, it is not suitable for either transportation applications that require good structural durability against shock and vibration or large-scale manufacturing because of its poor mechanical strength. The thickness of the graphite plates cannot be reduced, resulting in bulkiness and heaviness. As a result, recent studies have moved away from graphite in the direction of developing and optimizing more cost effective materials such as metals and composites.

Metallic materials are another choice for bipolar plates because of their good mechanical strength, high electrical conductivity, high thermal conductivity, high gas impermeability, low cost, and ease of manufacturing. The most advantage of metallic bipolar plates is stampability and reducing the thickness plate. Metallic bipolar plates can significantly reduce the volume of fuel cell stacks. In addition, relatively simple fabrication process of gas channels on the metallic plates by stamping enables mass production. In spite of these technical benefits, metallic plates are highly susceptible to corrosion which is closely related to reliability and durability of fuel cell engines. Recently, polymerecarbon composite bipolar plates have been investigated due to their lower cost, less weight, and higher corrosion resistivity in comparison with available materials such as graphite or metallic bipolar plates. The disadvantages of composite bipolar plates are non-stampability, lower electrical and mechanical properties than those of metallic bipolar plates. The effect of changing bipolar plate material are shown in Figures 15-18.

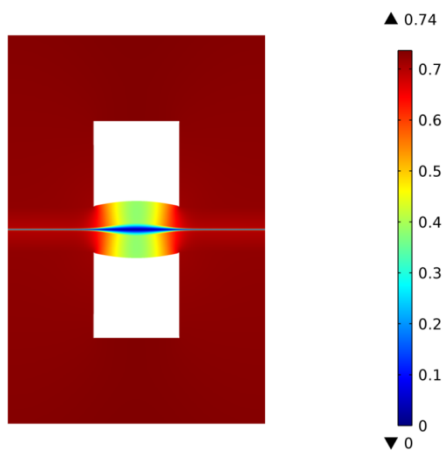


Figure 15. Total displacement [μm] in the PEM fuel cell during assembly process, (deformed shape plot, scale enlarged 200 times), (Metallic bipolar plate (SS316L): Young's modulus = 197 GPa; Density = 7800 kg/m³; Poisson's ratio = 0.3).

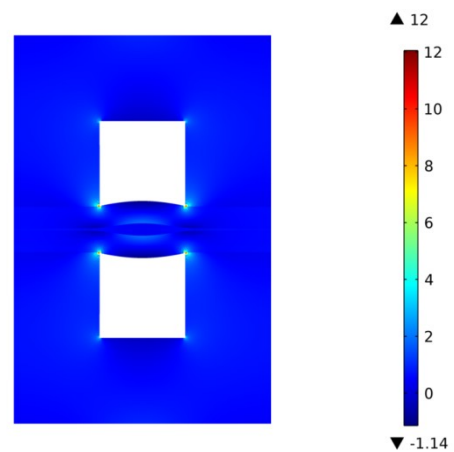


Figure 16. Pressure distribution [MPa] in the PEM fuel cell during assembly process, (deformed shape plot, scale enlarged 200 times), (Metallic bipolar plate (SS316L): Young's modulus = 197 GPa; Density = 7800 kg/m³; Poisson's ratio = 0.3).

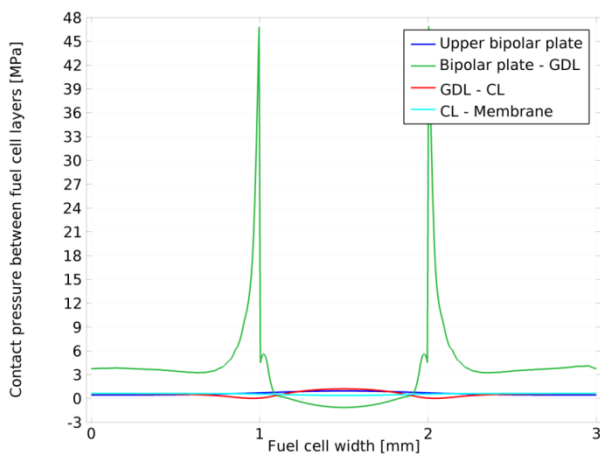


Figure 17. Contact pressure [MPa] between all layers of the fuel cell components during assembly process, (Metallic bipolar plate (SS316L): Young's modulus = 197 GPa; Density = 7800 kg/m³; Poisson's ratio = 0.3).

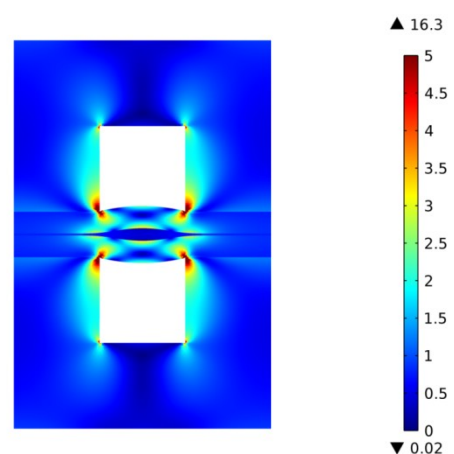


Figure 18. Mises stress distribution [MPa] in the PEM fuel cell during assembly process, (deformed shape plot, scale enlarged 200 times), (Metallic bipolar plate (SS316L): Young's modulus = 197 GPa; Density = 7800 kg/m³; Poisson's ratio = 0.3).

Each type of GDL material has its own optimal clamping pressure, to achieve a proper and uniform pressure distribution inside the cell. The inhomogeneous compression of the GDL leads to several opposing effects. On one hand, the assembly pressure improves both electric and thermal conductivities by reducing bulk and contact resistances. Slight compressions may also reduce mass transport resistance due to the shortening of the diffusion path to be covered by the reactants and products in their way to/from the catalyst layers. However, excessive compression loads may impede reactant and product transport due to the loss of pore volume, which is typically accompanied by a reduction of the effective species diffusivities. On top of that, excessive assembly pressures are known to damage typical paper type GDLs, induce local delamination of the GDL under the channel, and result in non-uniform compressive loads which may degrade the membrane. Pore size reduction may also affect multiphase capillary transport phenomena in the GDL (liquid water removal in PEM fuel cells). And last, but not least, partial GDL intrusion into the channel produces a reactant flow rate reduction, or, alternatively, an increase of the parasitic power required to maintain the flow, which affects the overall efficiency of the cell. The effect of changing GDL material are shown in Figures 19-22.

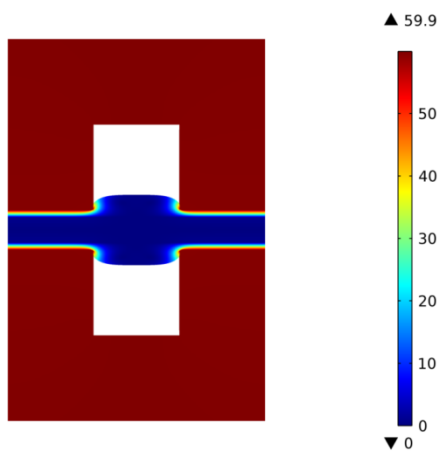


Figure 19. Total displacement [μm] in the PEM fuel cell during assembly process, (deformed shape plot, scale enlarged 3 times), (GDL (Toray TGP-H-030): Young's modulus = 0.0061 GPa; Density = 440 kg/m^3 ; Poisson's ratio = 0.1).

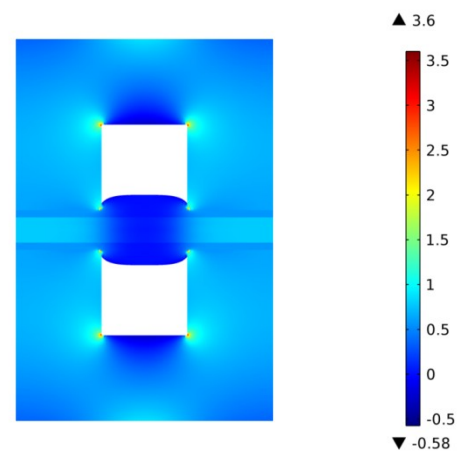


Figure 20. Pressure distribution [MPa] in the PEM fuel cell during assembly process, (deformed shape plot, scale enlarged 3 times), (GDL (Toray TGP-H-030): Young's modulus = 0.0061 GPa; Density = 440 kg/m^3 ; Poisson's ratio = 0.1).

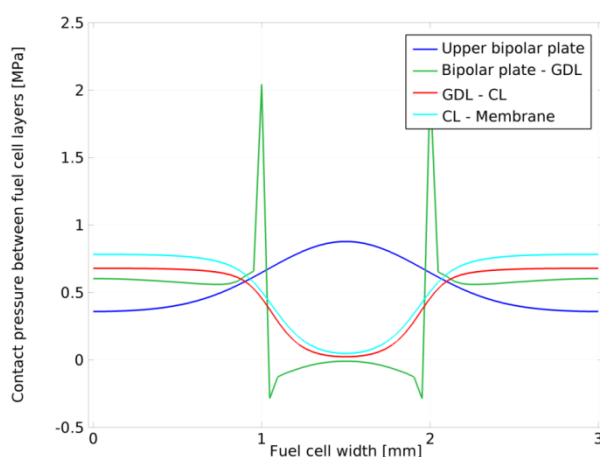


Figure 21. Contact pressure [MPa] between all layers of the fuel cell components during assembly process, (GDL (Toray TGP-H-030): Young's modulus = 0.0061 GPa; Density = 440 kg/m^3 ; Poisson's ratio = 0.1).

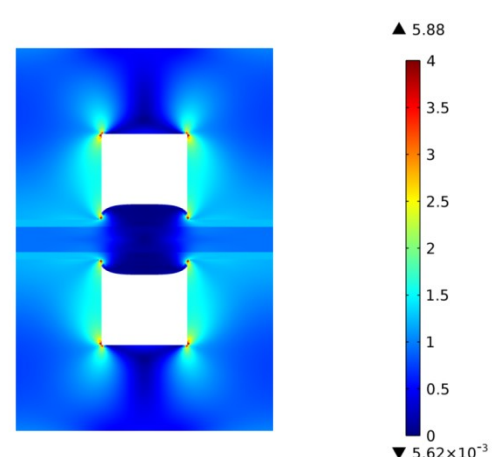


Figure 22. Mises stress distribution [MPa] in the PEM fuel cell during assembly process, (deformed shape plot, scale enlarged 3 times), (GDL (Toray TGP-H-030): Young's modulus = 0.0061 GPa; Density = 440 kg/m^3 ; Poisson's ratio = 0.1).

An important part of the fuel cell is the electrolyte, which gives every fuel cell its name. At the core of a PEM fuel cell is the polymer electrolyte membrane that separates the anode from the cathode. The desired characteristics of PEMs are high proton conductivity, good electronic insulation, good separation of fuel in the anode side from oxygen in the cathode side, high chemical and thermal stability, and low production cost. One type of PEMs that meets most of these requirements is Nafion[®]. Nafion[®] membranes come extruded in different sizes and thicknesses. They are marked with a letter N, followed by a 3- or 4-digit number. The first 2 digits represent equivalent weight divided by 100, and the last digit or two is the membrane thickness in mills. The protonic conductivity of a polymer membrane is strongly dependent on membrane structure and its water content. Water uptake results in the membrane swelling and changes its dimensions, which is a very significant factor for fuel cell design and assembly. The dimensional changes are in the order of magnitude of 10%, which must be taken into account in cell design and during the installation of the membrane in the cell. The thickness of the membrane is also important, since a thinner membrane reduces the ohmic losses in a cell. However, if the membrane is too thin, hydrogen, which is much more diffusive than oxygen, will be allowed to cross-over to the cathode side and recombine with the oxygen without providing electrons for the external circuit. The effect of changing membrane material are shown in Figures 23-26.

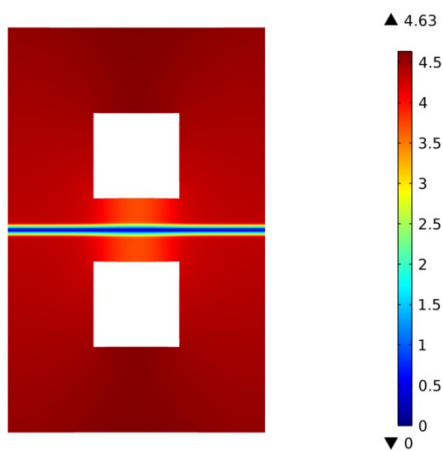


Figure 23. Total displacement [μm] in the PEM fuel cell during assembly process, (deformed shape plot, scale enlarged 10 times), (Membrane: Young's modulus = 0.02 GPa; Density = 918 kg/m^3 ; Poisson's ratio = 0.33).

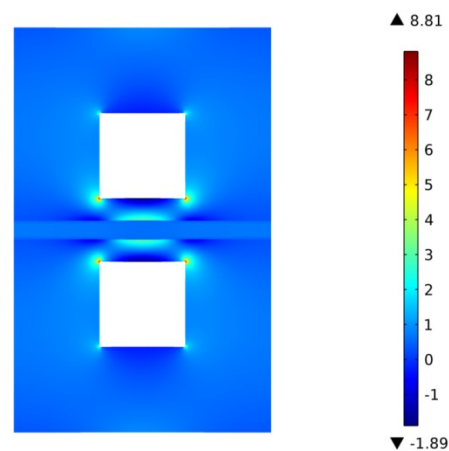


Figure 24. Pressure distribution [MPa] in the PEM fuel cell during assembly process, (deformed shape plot, scale enlarged 10 times), (Membrane: Young's modulus = 0.02 GPa; Density = 918 kg/m^3 ; Poisson's ratio = 0.33).

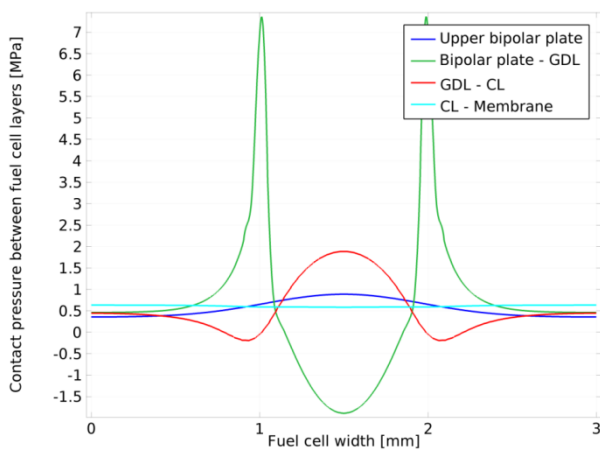


Figure 25. Contact pressure [MPa] between all layers of the fuel cell components during assembly process, (Membrane: Young's modulus = 0.02 GPa; Density = 918 kg/m^3 ; Poisson's ratio = 0.33).

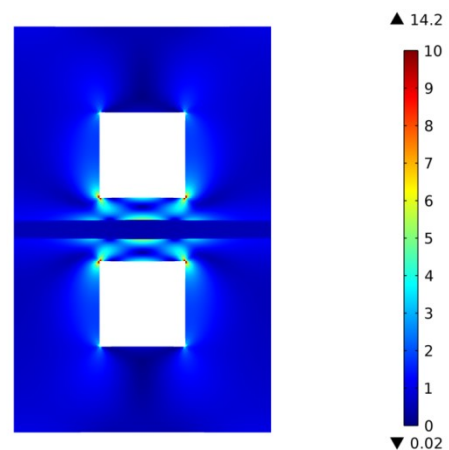


Figure 26. Mises stress distribution [MPa] in the PEM fuel cell during assembly process, (deformed shape plot, scale enlarged 10 times), (Membrane: Young's modulus = 0.02 GPa; Density = 918 kg/m^3 ; Poisson's ratio = 0.33).

The catalyst layer is the layer where the electrochemical reactions take place. More precisely, the electrochemical reactions take place on the catalyst surface. Because there are three kinds of species that participate in the electrochemical reactions, namely gases, electrons and protons, the reactions can take place on a portion of the catalyst surface where all three species have access. Electrons travel through electrically conductive solids, including the catalyst itself, but it is important that the catalyst particles are somehow electrically connected to the substrate. Protons travel through ionomer; therefore the catalyst must be in intimate contact with the ionomer. And finally, the reactant gases travel only through voids; therefore the electrode must be porous to allow gases to travel to the reaction sites. At the same time, product water must be effectively removed; otherwise the electrode would flood and prevent oxygen access. Several methods of applying the catalyst layer to the gas diffusion electrode have been reported. These methods are spreading, spraying, and catalyst power deposition. For the spreading method, a mixture of carbon support catalyst and electrolyte is spread on the GDL surface by rolling a metal cylinder on its surface. In the spraying method, the catalyst and electrolyte mixture is repeatedly sprayed onto the GDL surface until a desired thickness is achieved. The effect of changing CL material are shown in Figures 27-30.

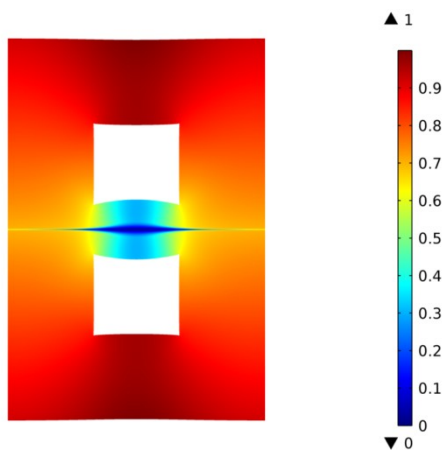


Figure 27. Total displacement [μm] in the PEM fuel cell during assembly process, (deformed shape plot, scale enlarged 200 times), (CL: Young's modulus = 0.249 GPa; Density = 1000 kg/m^3 ; Poisson's ratio = 0.3).

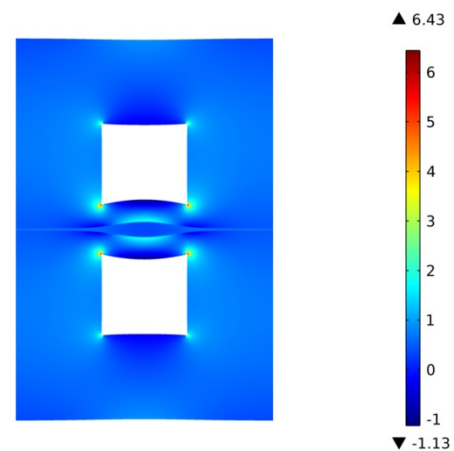


Figure 28. Pressure distribution [MPa] in the PEM fuel cell during assembly process, (deformed shape plot, scale enlarged 200 times), (CL: Young's modulus = 0.249 GPa; Density = 1000 kg/m^3 ; Poisson's ratio = 0.3).

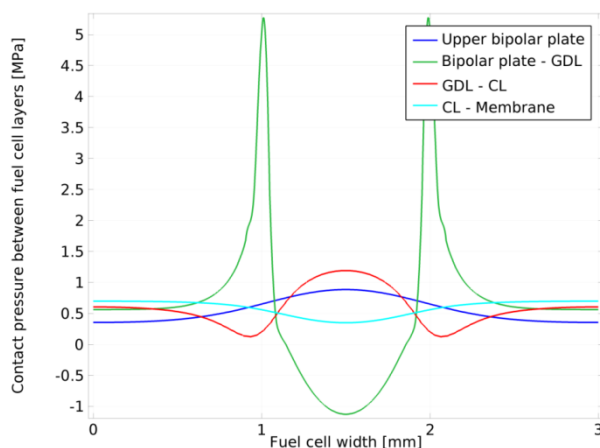


Figure 29. Contact pressure [MPa] between all layers of the fuel cell components during assembly process, (CL: Young's modulus = 0.249 GPa; Density = 1000 kg/m^3 ; Poisson's ratio = 0.3).

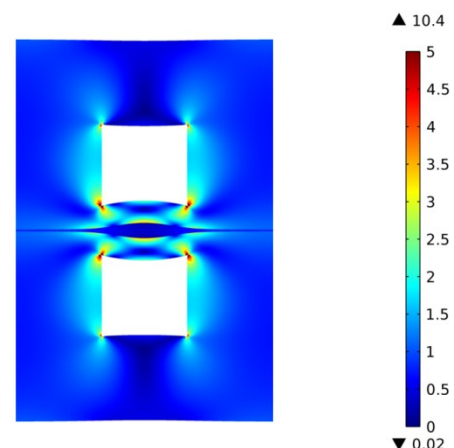


Figure 30. Mises stress distribution [MPa] in the PEM fuel cell during assembly process, (deformed shape plot, scale enlarged 200 times), (CL: Young's modulus = 0.249 GPa; Density = 1000 kg/m^3 ; Poisson's ratio = 0.3).

4.1.3. Effect of misalignment during assembly process

In practice, multiple single cells are usually connected in series to form a PEM fuel cell stack to provide the sufficient power and desired voltage. This configuration results in a high requirement of assembly accuracy for the adjacent bipolar plates. Otherwise, the assembly error will affect the perfect alignment of the adjacent bipolar plates and there will be an assembly position deviation, which leads to the assembly force transmitting asymmetrically and in turn makes the contact pressure distribution between the bipolar plate and MEA non-uniform. Moreover, such assembly error brings an extra moment to the MEA, which may deform the MEA seriously and produce stress concentration even cracks. Once the stress of MEA exceeds its yield strength, the plastic deformation will happen, and in turn, results in residual stresses in MEA after unloading, which are believed to be a significant contributor for the stress failure of MEA. Hence, it is very important to control the assembly error of the Bipolar plate to a low level in order to maintain a proper pressure distribution and avoid stress failure of the MEA.

However, the assembly error for the PEM fuel cell stack has not received enough attention currently, and in particular manual assembly processes are still widely applied for most of the stacks, which results in large assembly errors of the bipolar plates. Furthermore, during the running of a PEM fuel cell stack, the unavoidable vibration may aggravate the assembly error, especially for the automotive application due to more vibrations [10]. In addition, for the PEM fuel cell stack of metallic bipolar plate, the bipolar plate exhibits larger manufacturing error because of its plastic characters (for example spring-back), which in turn makes the influence of assembly error more serious.

On one hand, the assembly error of bipolar plate should be controlled and decreased in order to improve the performance of the PEM fuel cell. On the other hand, based on the current assembly process and manufacturing process, it is very hard to control the assembly error to a very low level. And moreover if the assembly error required is too small, the assembly and manufacturing cost of the PEM fuel cell stack will increase dramatically, which is unacceptable and conflict with the cost reduction of the PEM fuel cell. Therefore, there is a need to investigate the effect of the assembly error of the bipolar plate on the contact behaviour of PEM fuel cell in order to guide the assembly process, and furthermore obtain a trade-off between the performance and the assembly accuracy.

An example result of the misalignment (the channel alignment of the bipolar plate on the anode side is not be in the perfect match of the channel on the cathode side) during the process of fuel cell assembly are shown in Figures 31-34.

4.2. PEM fuel cell analysis during operation

The solid mechanics model which is discussed in previous section has been incorporated into full three-dimensional, multi-phase, non-isothermal computational fluid dynamics model of a proton exchange membrane fuel cell. The three-dimensional CFD model of a PEM fuel cell that used with the present solid mechanics model was developed, validated, and discussed in detail by the current author in his previous works [1-10]. In brief, the model is based on the computational fluid dynamics method and considers multi-phase, multi-component flow inside the gas flow channels and the porous media of a PEM fuel cell with straight flow channels. The model accounts for both gas and liquid phase in the same computational domain, and thus allows for the implementation of phase change inside the gas diffusion layers. The model includes the transport of gaseous species, liquid water, protons, energy, and water dissolved in the ion-conducting polymer. Water transport inside the porous gas diffusion layer and catalyst layer is described by two physical mechanisms: viscous drag and capillary pressure forces, and is described by advection within the gas channels. Water transport across the membrane is also described by two physical mechanisms: electro-osmotic drag and diffusion. Water is assumed to be exchanged among three phases; liquid, vapour, and dissolved, and equilibrium among these phases is assumed. This model takes into account convection and diffusion of different species in the channels as well as in the porous gas diffusion layer, heat transfer in the solids as well as in the gases, and electrochemical reactions. The model reflects the influence of the operating parameters on fuel cell performance to investigate the in situ total displacement and degree of the deformation of the polymer membrane of PEM fuel cells.

The cell operates at nominal current density of 1.2 A/cm^2 , air/fuel inlet pressure and temperature of 3 atm and 353.15 K respectively. The selection of relatively high current density is due to illustrate the membrane swelling and thermal stresses which are more visible in the cell in the high loading conditions. Figure 35 shows the temperature profile values correspond to the above operating conditions of a PEM fuel cell. The humidity is modeled as a constant RH value through the membrane (uniform loading). The

initial relative humidity of the membrane is taken as 30%, and then increased to 100% to simulate operating conditions. The membrane humidity swelling-expansion coefficient can be calculated from the experimental data of the swelling strain of the membrane as a function of humidity and temperature (Figure 36). All other parameters are at the base case conditions as outlined in Table 1.

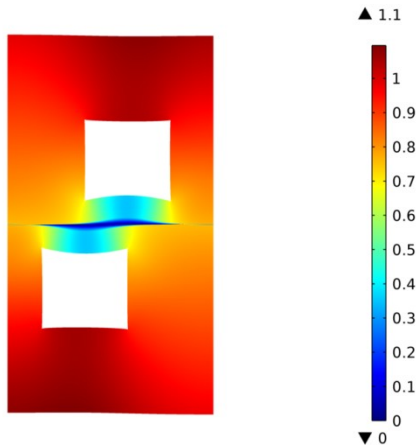


Figure 31. Total displacement [μm] in the PEM fuel cell during assembly process, (deformed shape plot, scale enlarged 200 times), assembly error effects.

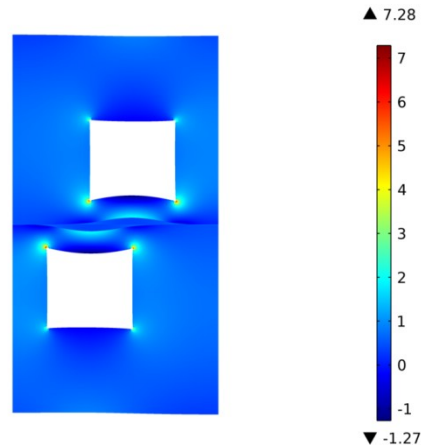


Figure 32. Pressure distribution [MPa] in the PEM fuel cell during assembly process, (deformed shape plot, scale enlarged 200 times), assembly error effects.

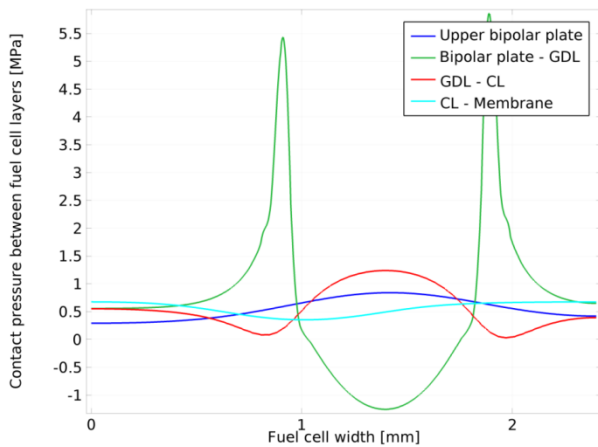


Figure 33. Contact pressure [MPa] between all layers of the fuel cell components during assembly process, assembly error effects.

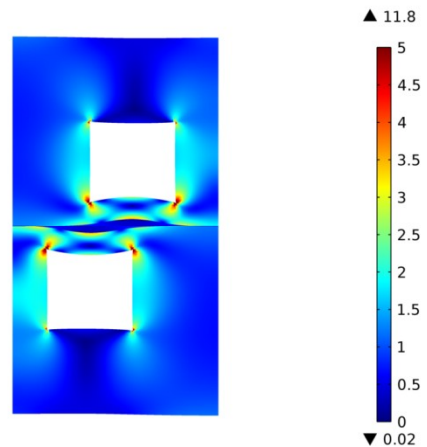


Figure 34. Mises stress distribution [MPa] in the PEM fuel cell during assembly process, (deformed shape plot, scale enlarged 200 times), assembly error effects.

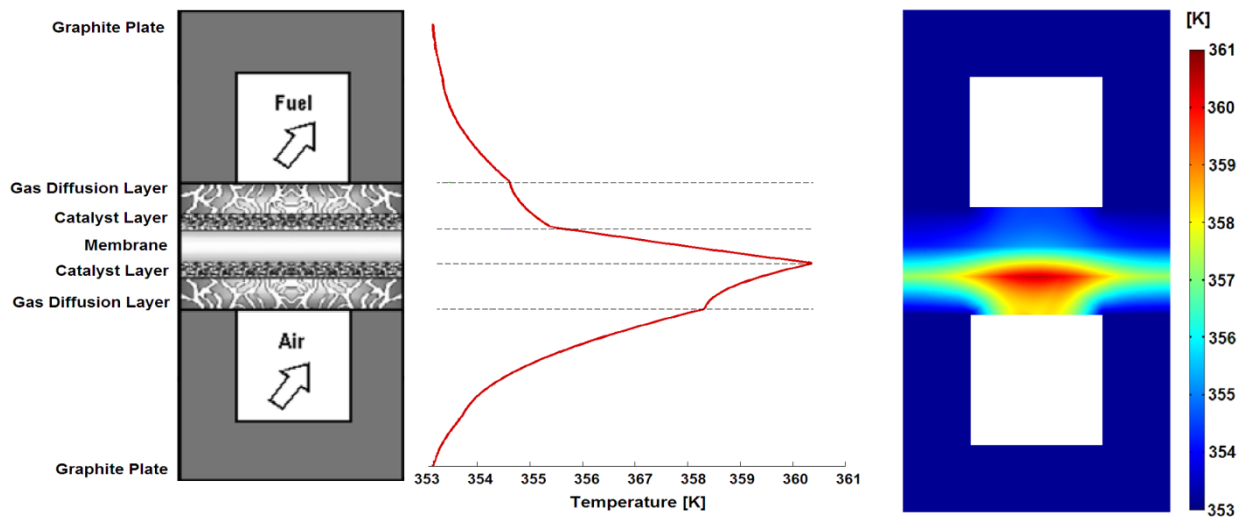


Figure 35. Temperature profile values correspond to the base case operating conditions of a PEM fuel cell.

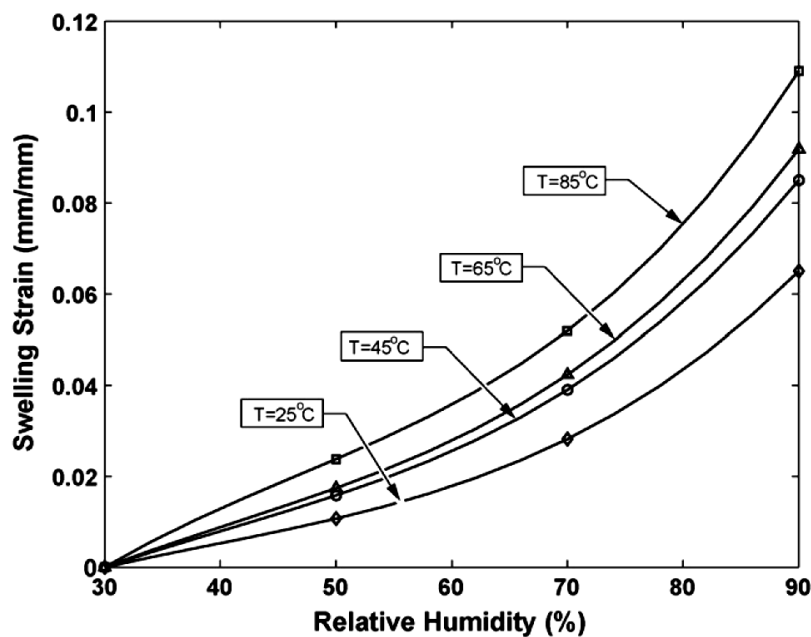


Figure 36. Experimental data (markers) for the swelling expansion in the membrane and the polynomial curve fit (solid lines) to these data points as a function of humidity and temperature, plotted for four constant temperatures for Nafion[®] [19].

Figures 37-40 showing the analysis of the PEM fuel cell during operation. The clamping pressure of 1 MPa are used as the base case assembly conditions. In overall, the results show high deformation, high pressure, and high stresses in the fuel cell components. This is due to the more pressure producing from the thermal expansion of the fuel cell materials and membrane swelling during cell operation.

Figure 37. shows the distribution of the total displacement in the PEM fuel cell during operation. The figure is clearly explain the effect of the repetitive channel-rib pattern on the pressure distribution.

The pressure distribution in the fuel cell that developed during both effects of the assembly process and operation can be seen in Figure 38. The figure shows pressure distribution (contour plots) and deformation shape for the fuel cell components.

In the operation PEM fuel cell, the contact pressure on the GDL is increased because of the thermal expansion of cell materials and membrane swelling. Furthermore, due to the round corners of the bipolar plate, the contact behaviour at the interface is hard to predict without a CFD analysis. Figure 39. shows the contact pressure between all layers of the fuel cell components during operation. The figure shows high contact pressure. This is due to the more pressure producing from the thermal expansion of the fuel cell materials and membrane swelling during cell operation.

The stresses distribution in the PEM fuel cells is affected by operating point (cell voltage and related current density). The stresses distribution in the fuel cell that developed during the cell operating can be seen in Figure 40. The figure shows von Mises stress distribution (contour plots) and deformation shape for the fuel cell. Because of the different thermal expansion and swelling coefficients between gas diffusion layers and membrane materials with non-uniform temperature distributions in the cell during operation, hygro-thermal stresses and deformation are introduced. The non-uniform distribution of stress, caused by the temperature gradient in the fuel cell, induces localized bending stresses, which can contribute to delaminating between the membrane and the GDLs. It can be seen that the maximum stress occurs, where the temperature is highest, which is near the cathode side inlet area. The maximum stress appears in the lower surface of membrane (cathode side), implying that major heat generation takes place near this region. The deformation that occurs in membrane under the land areas is much smaller than under the channel areas due to the clamping force effect.

Figure 41. illustrates the changes suffered by the porosity field during the compression process as a result of assembly process of the fuel cell, and also as a result of membrane swelling, and cell materials expansion due to the temperature and relative humidity cycles during operation. The GDL intrusion into the channel and the compressive stress applied at the rib symmetry plane are also indicated for illustrative purposes. The inhomogeneity associated with the repetitive channel-rib pattern is perfectly reflected, showing a region of large porosity reduction under the rib, a region of unperturbed porosity under the channel, and an intermediate fan like transition region below the channel-rib wall. Note in particular the accumulation of stresses under the rib corner, which results in high porosity reduction in this particular region. The simulations also show that the upper edge of the GDL experiences slight tensile strains in the region below the channel, thereby increasing the GDL porosity above its initial value 0.4.

In a real PEM fuel cell, the contact pressure on the GDL is different from the clamping pressure because of the channels in the bipolar plate. Furthermore, due to the round corners of the bipolar plate, the contact behaviour at the interface is hard to predict without a CFD analysis. Figure 42 shows the interfacial contact resistance along the rib width.

The most commonly used fuel cell configuration is the bipolar configuration. The membrane electrode assemblies and the bipolar plates need to be fixed in accurate positions. Otherwise, the assembly error will affect the perfect alignment of the adjacent bipolar plates and there will be an assembly position deviation. The assembly error has a significant effect on the uniformity of the pressure distribution and maximum Von Mises stress in the PEM fuel cell as be shown in the previous section. Therefore, the assembly error of bipolar plate should be controlled and decreased in order to improve the performance and durability of the operating PEM fuel cell. Figure 43-46 show the error effects on the PEM fuel cell during operation at the base case conditions.

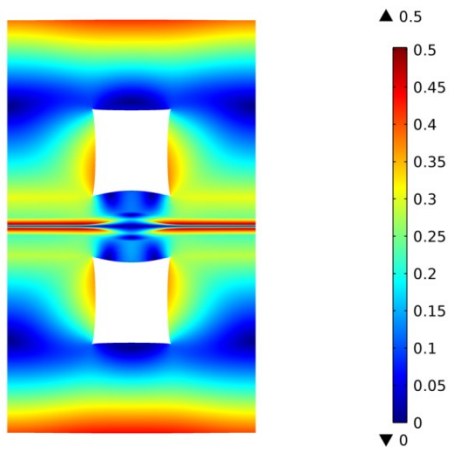


Figure 37. Total displacement [μm] in the PEM fuel cell during operation, (deformed shape plot, scale enlarged 200 times).

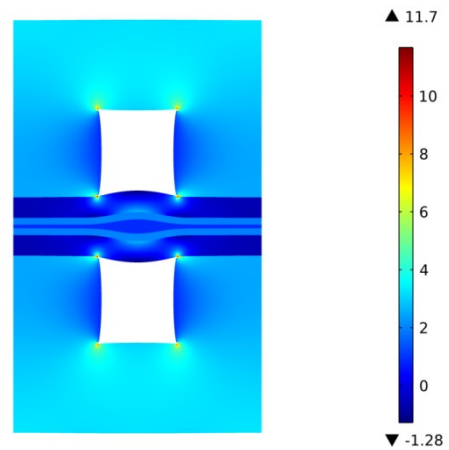


Figure 38. Pressure distribution [MPa] in the PEM fuel cell during operation, (deformed shape plot, scale enlarged 200 times).

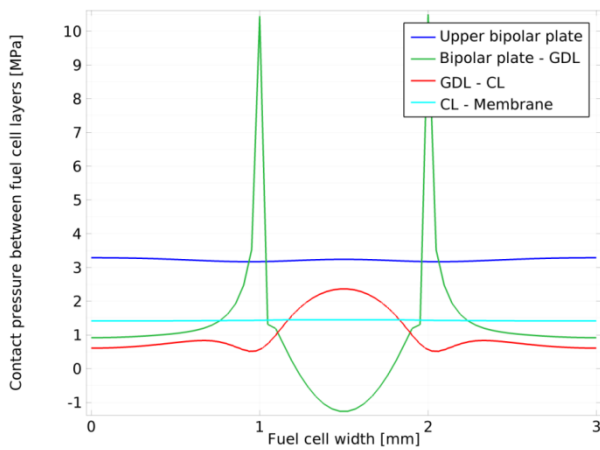


Figure 39. Contact pressure [MPa] between all layers of the fuel cell components during operation.

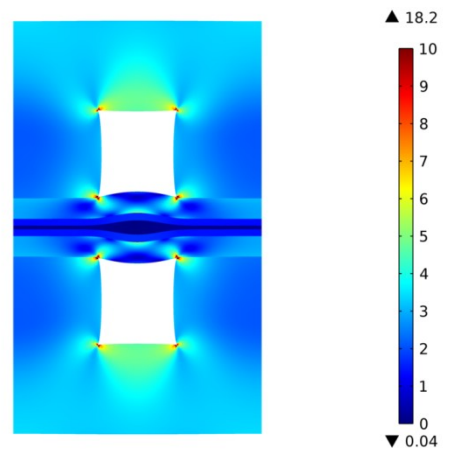


Figure 40. Mises stress distribution [MPa] in the PEM fuel cell during operation, (deformed shape plot, scale enlarged 200 times).

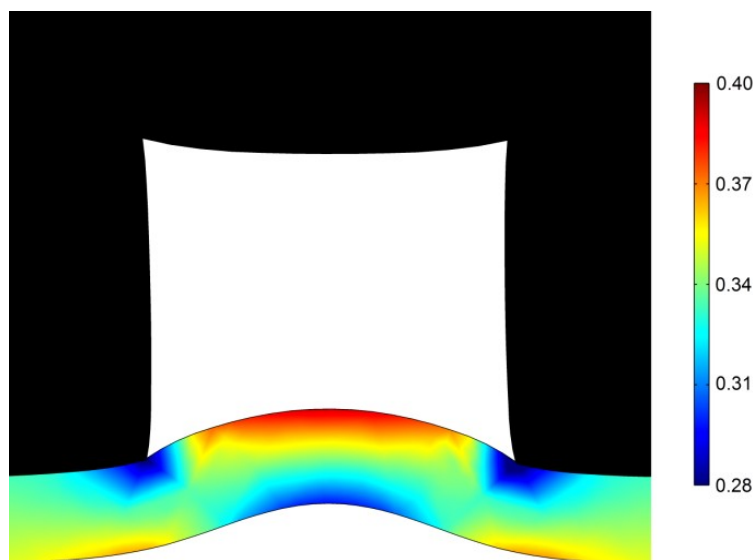


Figure 41. Porosity distribution in the GDLs (contour) and total displacement during operation, (deformed shape plot, scale enlarged 250 times).

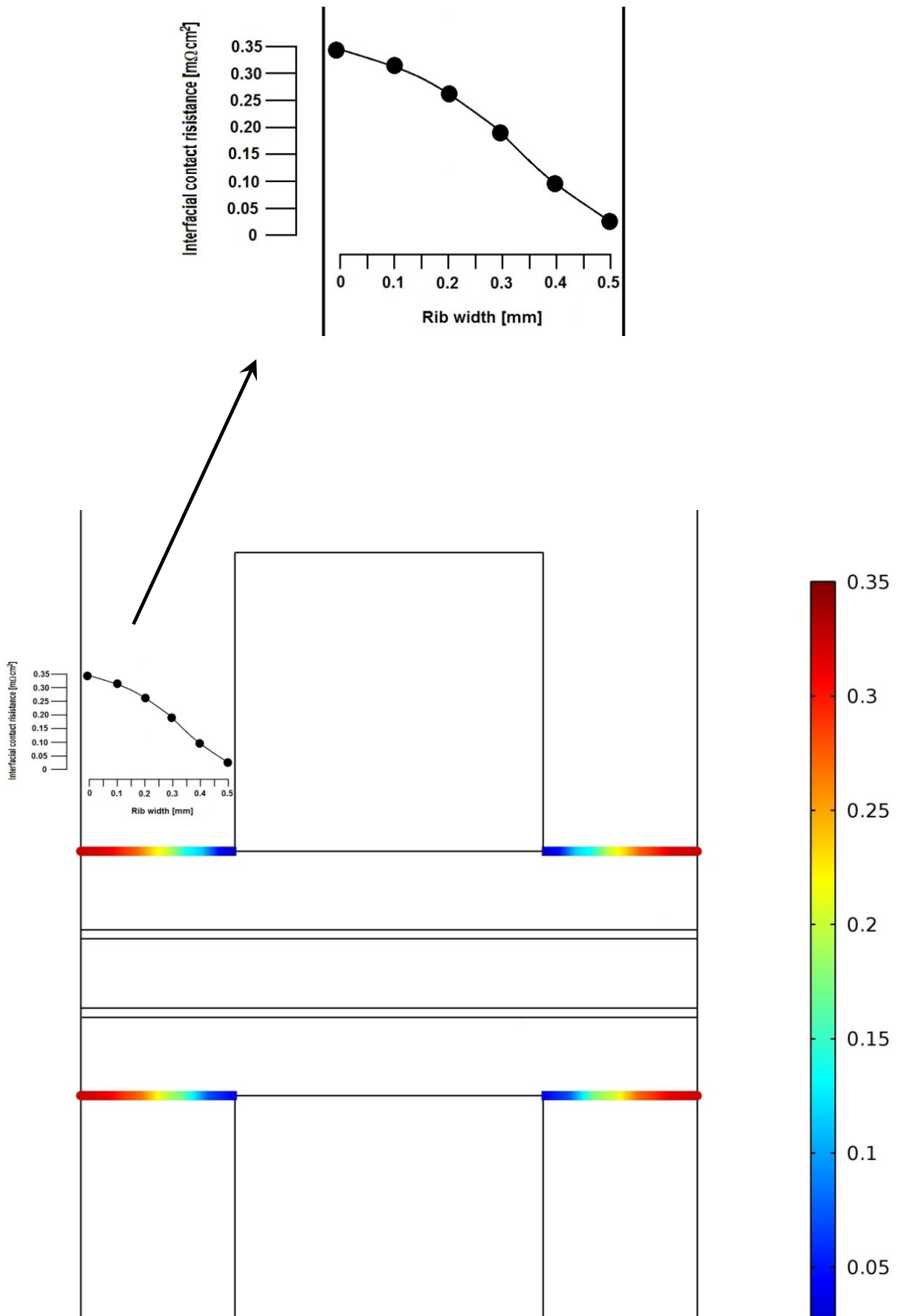


Figure 42. Interfacial contact resistance GDL/bipolar plate along the rib width.

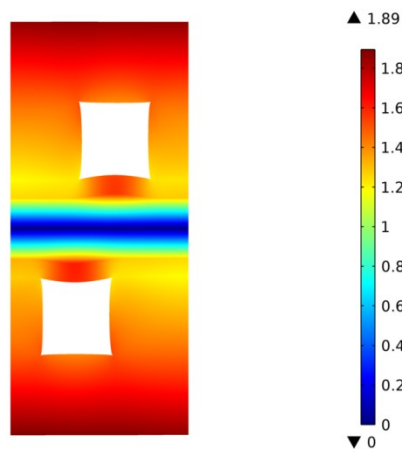


Figure 43. Total displacement [μm] in the PEM fuel cell during operation, (deformed shape plot, scale enlarged 200 times), assembly error effects.

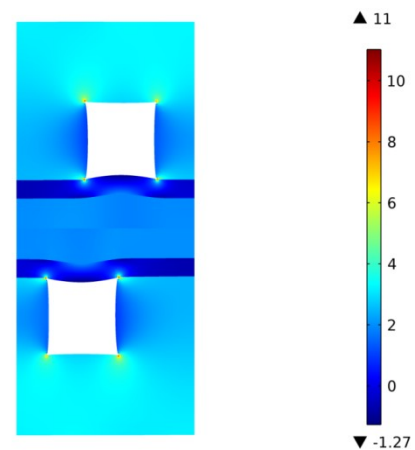


Figure 44. Pressure distribution [MPa] in the PEM fuel cell during operation, (deformed shape plot, scale enlarged 200 times), assembly error effects.

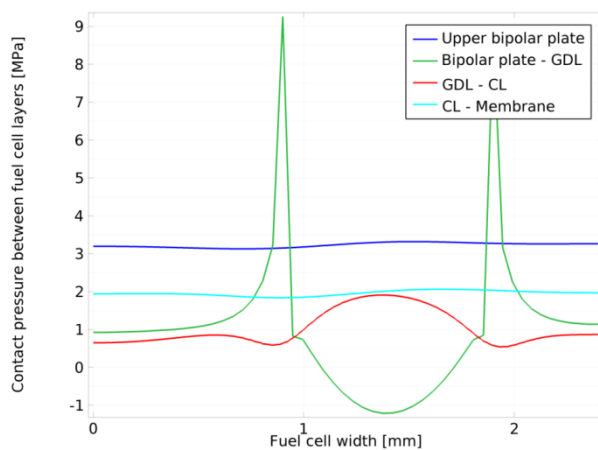


Figure 45. Contact pressure [MPa] between all layers of the fuel cell components during operation, assembly error effects.

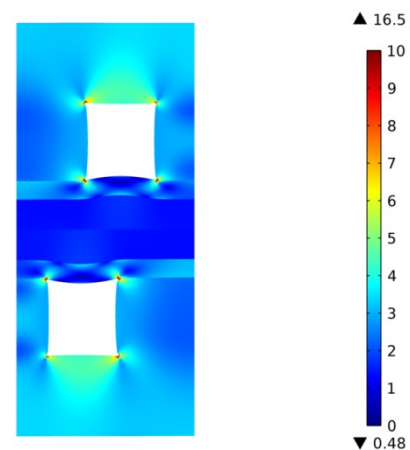


Figure 46. Mises stress distribution [MPa] in the PEM fuel cell during operation, (deformed shape plot, scale enlarged 200 times), assembly error effects.

5. Conclusion

Many parameters must be considered when designing a PEM fuel. Some of the most basic design considerations include power required, size, weight, volume, cost, transient response, and operating conditions.

PEM fuel cell assembly process, including clamping pressure, material properties of each component, and design (component thickness and cell active area) are important factors influencing the performance and durability of the PEM fuel cell. Furthermore, when temperature and relative humidity increase during operation, the membrane absorbs water and swells. Since the relative position between the top and bottom end plates is fixed, the polymer membrane is spatially confined. Thus the GDL will be further compressed under the land and the intrusion into channel becomes more significant. Assembly pressure, contact resistance, membrane swelling and operating conditions, etc., combine to yield an optimum assembly pressure. The clamping pressure is therefore a critical parameter for optimal fuel cell performance and durability. Too high, too low, or inhomogeneous compressions have negative effects on the performance and durability of the fuel cells.

The most commonly used stack configuration is the bipolar configuration. The membrane electrode assemblies and the bipolar plates need to be fixed in accurate positions. Otherwise, the assembly error will affect the perfect alignment of the adjacent bipolar plates and there will be an assembly position

deviation. The assembly error has a significant effect on the uniformity of the pressure distribution and maximum Von Mises stress in the PEM fuel cell. Therefore, the assembly error of bipolar plate should be controlled and decreased in order to improve the performance and durability of the PEM fuel cell.

References

- [1] Maher A.R. Sadiq Al-Baghdadi. CFD models for analysis and design of PEM fuel cells. Nova Science Publishers 2008, ISBN: 978160456-9971.
- [2] Maher A.R. Sadiq Al-Baghdadi. CFD modeling and analysis of different novel designs of air-breathing PEM fuel cells. Nova Science Publishers 2010, ISBN: 9781608764891.
- [3] Maher A.R. Sadiq Al-Baghdadi. PEM Fuel Cells Fundamentals, Modeling and Applications. International Energy and Environment Foundation 2013, ISBN: 9781481978231.
- [4] Maher A.R. Sadiq Al-Baghdadi. Optimal design of PEM fuel cells to generate maximum power: A CFD study. International Journal of Energy and Environment, 2011; 2(6), 953-962.
- [5] Maher A.R. Sadiq Al-Baghdadi. Mechanical behaviour of PEM fuel cell catalyst layers during regular cell operation. International Journal of Energy and Environment, 2010; 1(6), 927-936.
- [6] Maher A.R. Sadiq Al-Baghdadi. A CFD analysis on the effect of ambient conditions on the hygro-thermal stresses distribution in a planar ambient air-breathing PEM fuel cell. International Journal of Energy and Environment, 2011; 2(4), 589-604.
- [7] Maher A.R. Sadiq Al-Baghdadi. Modeling optimizes PEM fuel cell durability using three-dimensional multi-phase computational fluid dynamics model. International Journal of Energy and Environment IJEE, 2010; 1(3), 375-398.
- [8] Maher A.R. Sadiq Al-Baghdadi. Novel design of a compacted micro-structured air-breathing PEM fuel cell as a power source for mobile phones. International Journal of Energy and Environment IJEE, 2010; 1(4), 555-572.
- [9] Maher A.R. Sadiq Al-Baghdadi. Novel design of a disk-shaped compacted micro-structured air-breathing PEM fuel cell. International Journal of Energy and Environment, 2012; 3(2), 161-180.
- [10] Maher A.R. Sadiq Al-Baghdadi. Prediction of deformation and hygro-thermal stresses distribution in PEM fuel cell vehicle using threedimensional CFD model. International Journal of Energy and Environment IJEE, 2012; 3(4), 485-504.
- [11] Zhang, S.; Yuan, X.; Wang, H.; Merida, W.; Zhu, H.; Shen, J.; Wu, S.; Zhang, J. A review of accelerated stress tests of MEA durability in PEM fuel cells. Int. J. Hydrogen Energy, 2009; 34(1): 388-404.
- [12] Wu, J.; Yuan, X.Z.; Martin, J.J.; Wang, H.; Zhang, J.; Shen, J.; Wu, S.; Merida, W. A review of PEM fuel cell durability: Degradation mechanisms and mitigation strategies. J. Power Sources, 2008; 184(1): 104-119.
- [13] Beuscher, U.; Cleghorn, S.J.C.; Johnson, W.B. Challenges for PEM fuel cell membranes. Int. J. Energy Res. 2005; 29(12): 1103-1112.
- [14] Gode, P.; Ihonen, J.; Strandroth, A.; Ericson, H.; Lindbergh, G.; Paronen, M.; Sundholm, F.; Sundholm, G.; Walsby, N. Membrane durability in a pem fuel cell studied using PVDF based radiation grafted membranes fuel cells. Fuel Cells 2003; 3(1-2): 21-27.
- [15] Crum, M.; Liu, W. Effective Testing Matrix for Studying Membrane Durability in PEM Fuel Cells. Part 2. Mechanical Durability and Combined Mechanical and Chemical Durability, vol. 3. Electrochemical Society Inc., Pennington, NJ 08534-2896, United States, Cancun, Mexico, 2006: 541-550.
- [16] Marrony, M.; Barrera, R.; Quenet, S.; Ginocchio, S.; Montelatichi, L.; Aslanides, A. Durability study and lifetime prediction of baseline proton exchange membrane fuel cell under severe operating conditions. J. Power Sources, 2008; 182(2): 469-475.
- [17] Stanic V, Hoberech M. Mechanism of pin-hole formation in membrane electrode assemblies for PEM fuel cells. Electrode Assemblies for PEM Fuel Cells, Electrochemical Society Inc., Pennington, NJ 08534-2896, United States, Honolulu, HI, United States, 2004; p. 1891.
- [18] Ramaswamy, N.; Hakim, N.; Mukerjee, S. Degradation mechanism study of perfluorinated proton exchange membrane under fuel cell operating conditions. ElectrochimicaActa 2008; 53(8): 3279-3295.
- [19] Tang Y, Karlsson AM, Santare MH, Gilbert M, Cleghorn S, Johnson WB. An experimental investigation of humidity and temperature effects on the mechanical properties of perfluorosulfonic acid membrane. J. Mater Sci. Eng. 2006; 425(1-2): 297-304.

- [20] Xie J, Wood DL, Wayne DM, Zawodzinski T, Borup RL. Durability of polymer electrolyte fuel cells at high humidity conditions. *J. Electrochem. Soc.* 2005; 152(1): A104-A113.
- [21] Kim, S.; Mench, M.M. Investigation of temperature-driven water transport in polymer electrolyte fuel cell: phase-change-induced flow. *J. Electrochem. Soc.* 2009; 156(3): B353-B362.
- [22] Kim, S.; Mench, M.M. Investigation of temperature-driven water transport in polymer electrolyte fuel cell: Thermo-osmosis in membranes. *J. Membrane Sci.* 2009; 328(1-2): 113-120.
- [23] Berning, T.; Lu, D.M.; Djilali, N. Three-dimensional computational analysis of transport phenomena in a PEM fuel cell. *J. Power Sources*, 2002; 106(1-2): 284-294.
- [24] Berning, T.; Djilali, N. Three-dimensional computational analysis of transport phenomenon in a PEM fuel cell-a parametric study. *J. Power Sources*, 2003; 124(2): 440-452.
- [25] Sivertsen, B.R.; Djilali, N. CFD based modelling of proton exchange membrane fuel cells. *J. Power Sources*, 2005; 141(1): 65-78.
- [26] Webber, A.; Newman, J.A. Theoretical study of membrane constraint in polymer-electrolyte fuel cell. *AIChE J.*, 2004; 50(12): 3215-3226.
- [27] Tang, Y.; Santare, M.H.; Karlsson, A.M.; Cleghorn, S.; Johnson, W.B. Stresses in proton exchange membranes due to hygro-thermal loading. *J. Fuel Cell Sci.andTech. ASME*, 2006; 3(5): 119-124.
- [28] Kusoglu, A; Karlsson, A.M.; Santare, M.H.; Cleghorn, S; Johnson, W.B. Mechanical response of fuel cell membranes subjected to a hygro-thermal cycle. *J. Power Sources*, 2006; 161(2): 987-996.
- [29] Kusoglu, A.; Karlsson, A.M.; Santare, M.H.; Cleghorn, S.; Johnson, W.B. Mechanical behavior of fuel cell membranes under humidity cycles and effect of swelling anisotropy on the fatigue stresses. *J. Power Sources*, 2007; 170(2): 345-358.
- [30] Solasi, R.; Zou, Y.; Huang, X.; Reifsnider, K.; Condit, D. On mechanical behavior and in-plane modeling of constrained PEM fuel cell membranes subjected to hydration and temperature cycles. *J. Power Sources*, 2007; 167(2): 366-377.
- [31] Bograchev, D.; Gueguen, M.; Grandidier, J-C.; Martemianov, S. Stress and plastic deformation of MEA in fuel cells stresses generated during cell assembly. *J. Power Sources*, 2008; 180(2): 393-401.
- [32] Suvorov, A.P.; Elter, J.; Staudt, R.; Hamm, R.; Tudryn, G.J.; Schadler, L.; Eisman, G. Stress relaxation of PBI based membrane electrode assemblies. *Int. J. Solids and Structures*, 2008; 45(24): 5987-6000.
- [33] Tang, Y.; Kusoglu, A.; Karlsson, A.M.; Santare, M.H.; Cleghorn, S.; Johnson, W.B. Mechanical properties of a reinforced composite polymer electrolyte membrane and its simulated performance in PEM fuel cells. *J. Power Sources*, 2008; 175(2): 817-825.
- [34] Bograchev, D.; Gueguen, M.; Grandidier, J-C.; Martemianov, S. Stress and plastic deformation of MEA in running fuel cell. *Int. J. Hydrogen Energy*, 2008; 33(20): 5703-5717.
- [35] Maher A.R. Sadiq Al-Baghdadi. A CFD study of hygro-thermal stresses distribution in PEM fuel cell during regular cell operation. *Renewable Energy Journal* 2009; 34(3): 674-682.
- [36] Christophe Carral, Nicolas Charvin, Helene Trouve, Patrice Mele. An experimental analysis of PEMFC stack assembly using strain gage sensors. *Int. J. Hydrogen Energy* 2014, 39, 4493-4501.
- [37] I. Gatto, F. Urbani, G. Giacoppo, O. Barbera, E. Passalacqua. Influence of the bolt torque on PEFC performance with different gasket materials. *Int. J. Hydrogen Energy* 2011, 36, 13043-13050.
- [38] Thomas J. Mason, Jason Millichamp, Tobias P. Neville, Ahmad El-kharouf, Bruno G. Pollet, Daniel J.L. Brett. Effect of clamping pressure on ohmic resistance and compression of gas diffusion layers for polymer electrolyte fuel cells. *Journal of Power Sources* 2012, 219, 52-59.
- [39] DebanandSingdeo, TapobrataDey, Prakash C. Ghosh. Contact resistance between bipolar plate and gas diffusion layer in high temperature polymer electrolyte fuel cells. *Int. J. Hydrogen Energy* 2014, 39, 987-995.
- [40] RoshanakBanan, AimyBazylak, Jean Zu. Effect of mechanical vibrations on damage propagation in polymer electrolyte membrane fuel cells. *Int. J. Hydrogen Energy* 2013, 38, 14764-14772.
- [41] Z.Y. Su, C.T. Liu, H.P. Chang, C.H. Li, K.J. Huang, P.C. Sui. A numerical investigation of the effects of compression force on PEM fuel cell performance. *Journal of Power Sources* 2008, 183, 182-192.
- [42] C. Totzke, G. Gaiselmann, M. Osenberg, J. Bohner, T. Arlt, H. Markotter, A. Hilger, F. Wieder, A. Kupsch, B.R. Muller, M.P. Hentschel, J. Banhart, V. Schmidt, W. Lehnert, I. Manke. Three-

- dimensional study of compressed gas diffusion layers using synchrotron X-ray imaging. *Journal of Power Sources* 2014, 253, 123-131.
- [43] Kyung Don Baik, Bo Ki Hong, Kookil Han, Min Soo Kim. Effects of anisotropic bending stiffness of gas diffusion layers on the performance of polymer electrolyte membrane fuel cells with bipolar plates employing different channel depths. *Renewable Energy* 2014, 69, 356-364.
- [44] I. Nitta, S. Karvonen, O. Himanen, and M. Mikkola. Modelling the Effect of Inhomogeneous Compression of GDL on Local Transport Phenomena in a PEM Fuel Cell. *Fuel Cells* 2008, 410-421.